Pergamon

Continental Shelf Research, Vol. 15, No. 2/3, pp. 149–164, 1995

0278–4343/95 $9.50+0.00

0278–4343(94)E0023–F

Pb-210 fluxes and sedimentation rates on the lower continental slope between Taiwan and the South Okinawa Trough

Y. CHUNG* and W.C. CHANG*

(*Received* 12 *August* 1993; *accepted* 6 *January* 1994)

Abstract—Pb-210 and Ra-226 have been measured on 11 cores taken from the continental slope between northern Taiwan and the western South Okinawa Trough. Ra-226 activities generally fall between 0.5 and 2 dpm g^{-1}. Pb-210 activities are widely variable in these cores: negligible excess Pb-210 (or no Pb-210 flux) is observed on the upper and middle slope while large excess Pb-210 values (50–90 dpm g^{-1}) are present on the lower slope. Sedimentation rates estimated from the excess Pb-210 profiles of the cores range from 0.09 to 0.52 cm y^{-1} (0.08–0.42 g cm^{-2} y^{-1}) for the lower slope and decrease toward the deeper (eastern) slope.

Excess Pb-210 inventories and the Pb-210 fluxes calculated from the lower slope are 320–840 dpm cm^{-2} and 10–26 dpm cm^{-2} y^{-1}, respectively, assuming a steady-state input at each site for the past 100 years. Atmospheric input of Pb-210 and local production from Ra-226 do not account for the observed fluxes. Two alternative explanations are proposed: (1) boundary scavenging coupled with the Kuroshio water flowing through the area; or (2) downslope transport of high Pb-210 activity fine-grained particles from the shelf and upper/middle slope to the lower slope where they are deposited.

INTRODUCTION

ALTHOUGH marginal sediments around Taiwan have been studied in various aspects (e.g. BOGGS *et al.*, 1979; LIN and CHEN, 1983; CHEN, 1983), there are little data on sedimentation rates on the continental margin around Taiwan where high terrigenous particulate input is expected due to the extremely high denudation or erosion rates of the Island (LI, 1976). In the shelf and slope areas off western and southwestern Taiwan, where several major rivers discharge, recent Pb-210 data indeed show quite high sedimentation rates, ranging from 0.07 to 0.7 cm y^{-1} (TSAI and CHUNG, 1989). However, preliminary ^{14}C dating of piston-cored sediments in the Taiwan Strait indicates rates of only 0.004–0.015 cm y^{-1} (CHEN and COVEY, 1983).

Off northeastern Taiwan, the East China Sea continental shelf and the western South Okinawa Trough are linked with a continental slope. The Kuroshio current turns northeastward here due to the topographic barrier of the shelf and slope (LIU, 1983), which induces year-round upwelling caused by intrusion of Kuroshio subsurface water (LIU *et al.*, 1992). Mineralogical data (LIN and CHEN, 1983) suggest that the muddy sediments in the Okinawa Trough are mainly terrigenous deriving from China, Taiwan

*Institute of Marine Geology, National Sun Yat-sen University, Kaohsiung, Taiwan.

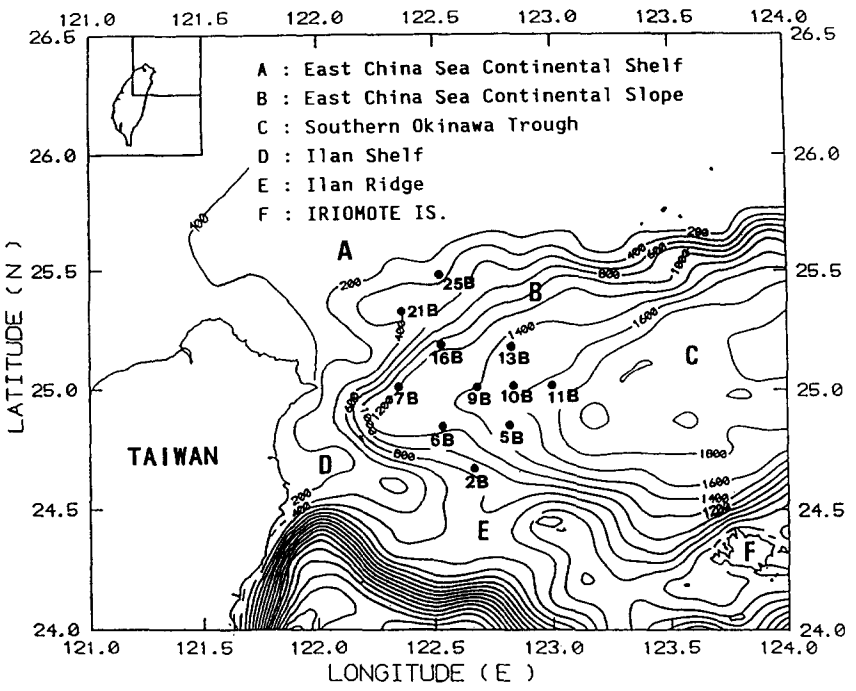

Fig. 1. Map showing bathymetry of the western South Okinawa trough and locations of the box cores studied. Contour intervals are 200 m except for that of the East China Sea Shelf which is 100 m.

and the Ryukyu Island Arc. As biogenous and volcanic contributions are quite small, LIN and CHEN (1983) conclude that the continent-derived sediments are transported and dispersed from the East China Sea by bottom currents. It is unknown whether the intervening slope is a conduit for East China Sea sediments given the regional bathymetry and Kuroshio-dominated current regime. In the present paper we employ Pb-210 geochronology to determine the rates of sedimentation on the northeastern Taiwan slope area to provide insight into the source, transport and flux of sediment to the lower slope.

Geologic setting

The study area is composed of three structural units (i.e. the East China Sea shelf, continental slope, and South Okinawa Trough, Fig. 1). South of the trough, the narrow Ilan Ridge separates the trough from the Nanau basin and extends eastward beyond Iriomote Island to merge with the Ryukyu Island Arc. Thus, tectonically, the Ilan Ridge is a western extension of the island arc below which the Philippine Sea plate subducts northward. The ridge connects with the Luzon volcanic arc in acute angle in northeastern Taiwan (Ho, 1986). During the last glaciation the East China Sea shelf was incised by river channels that discharged directly into the trough via the continental slope off northeastern Taiwan. The slope area between 400 and 1200 m depth exhibits erosional channels, slumping and turbidites due to its relative steepness and associated bottom currents (LIN, 1992; YU and HONG, 1992; CHEN *et al.*, 1992).

Table 1. *Location and water depth of the box cores used in this study. These cores were taken during Cruise* 281 *of the* Ocean Researcher I *in May* 1991

Core No.	Longitude (E)	Latitude (N)	Water Depth (m)
2B	122°39.29′	24°39.47′	669
5B	122°49.08′	24°50.18′	1522
6B	122°31.24′	24°49.08′	1306
7B	122°20.48′	25°00.19′	1187
9B	122°40.24′	24°59.44′	1465
10B	122°50.16′	25°00.17′	1518
11B	123°00.04′	25°00.03′	1608
13B	122°49.58′	25°11.06′	1512
16B	122°30.88′	25°11.35′	894
21B	122°21.28′	25°20.05′	696
25B	122°30.05′	25°29.83′	420

This slope area has been divided into three lithologic provinces by LIN (1992): an upper slope province that encompasses the shelf break and the slope shallower than 420 m deep, the middle slope (340–840 m), and the lower slope (below 900 m). The upper slope is covered with relict sediments of last glaciation (coarse sands or pebbles) and modern shell fragments. Mean grain size decreases downslope with organic-rich silts on the middle slope (LIN *et al.*, 1992) giving way to clayey silts and silty clays (carbonate ≦5%; sand ≦2%) on the lower slope.

METHODS

Field sampling

Twenty-six box cores were collected from the continental slope off northeastern Taiwan between 24°N and 26°N latitude, and 122°E and 124°E longitude during cruise 281 of the R.V. *Ocean Researcher I* in May, 1991. Eleven of the box cores were analyzed for Pb-210 and Ra-226 activities. Locations of these cores are shown in Fig. 1. Each box core was subcored as soon as it was recovered on deck by pushing 5 cm diameter PVC tubes gently into the sediment. Subcores were sealed and stored vertically in the ship freezer (−20°C) and transported to a shore-based laboratory, where they were sectioned with a stainless steel saw and subsampled at 2 cm depth intervals. Care was taken to remove the core surface in contact with the core liner and cutting surface from the sample to avoid possible contamination. Core locations and water depths are listed in Table 1.

Pb-210 *and* Ra-226 *measurements*

Aliquots of about 100 g from the subsamples were weighed before and after drying in oven at 110°C for 48 h to obtain water contents. Dried samples were ground, homogenized, and ashed at 550°C for 6 h. The weight loss due to ashing is designated in the paper as loss on ignition (LOI) which is a measure of organic matter and other volatiles.

Pb-210 techniques adopted for this study are after APPLEQUIST (1975) and TSAI and CHUNG (1989). Briefly, a $Pb(NO_3)_2$ carrier solution (equivalent to 300 mg of $PbSO_4$) was

added to each ashed sample of about 3–5 g and leached with 6 N HCl for 2 h on a hot plate. The cooled solution was filtered and the residue was leached for another 2 h. Following a second filtration, the combined filtrate was heated to dryness, dissolved in doubly distilled water (DDW), and then sufficient Na_2CrO_4 was added to precipitate the carrier Pb as $PbCrO_4$, which was collected by centrifugation. The $PbCrO_4$ precipitate was dissolved in 1.5 N HCl in a heated water bath. This solution was loaded onto an anion exchange column prepared with AG1-X8 mesh Cl^- form resin and pre-rinsed with 1.5 N HCl. Pb in the column was eluted with DDW at 70°C. The sample was heated to near dryness before adding a few drops of concentrated HNO_3 to precipitate $Pb(NO_3)_2$. The precipitate was then dissolved in DDW and converted to $PbSO_4$ precipitate by adding a few drops of concentrated H_2SO_4. The $PbSO_4$ was filtered and ashed at 550°C for at least 3 h to remove the ashless filter paper. After grinding, the $PbSO_4$ sample was uniformly deposited onto a circular disc (19.63 cm^2 area) using methanol as an adhesive. Samples were weighed to obtain chemical yields, which typically ranged between 50 and 80%.

Sample discs were stored for 1 month in a desiccator prior to counting Bi-210 activity in a low-background gas-flowing anti-coincidence beta counter, in order to allow ingrowth of Bi-210 to equilibrium with Pb-210. The counter was calibrated with a Pb-210 standard (~35 dpm) prepared by the Isotopes Product Loboratory of Burbank, California.

Ra-226 measurements were performed by the regenerated Rn-222 method which has been widely used for seawater samples and adopted as a standard by the GEOSECS program (e.g. BROECKER *et al.*, 1976; CHUNG and CRAIG, 1980; KU *et al.*, 1980. Ashed sediment samples were leached with 6 N HCl for 3 h on a hot plate. This leachate was filtered, diluted and stored in sealed 1-l glass bottles. After 1 month to allow Rn-222 to grow to equilibrium with Ra-226, the Rn-222 was extracted with He as a carrier gas using a radon stripping board used by the GEOSECS program (CHUNG and CRAIG, 1980). The Rn-222 extracted was transferred into a Lucas cell whose inner wall was coated with silver activated ZnS as a scintillator. The Lucas cell containing Rn-222 and its two alpha daughters, Po-218 and Po-214, was counted on a Pylon AB-5 alpha scintillation counter. Details on calibration and data reduction for this technique were given by CHUNG (1971).

RESULTS

Sediment character

Typical profiles of the water content (not corrected for salinity) and LOI of the box cores are shown in Fig. 2. Core 25B, located in the upper slope relict facies, has the lowest water content (25%) and LOI (4%), observed [Fig. 2(A)]. This core is about 70% sands and 30% pebbles, with abundant shell fragments. Cores 2B and 21B from the organic-rich silts with authigenic sulfides on the middle slope have a water content and LOI of about 40 and 7%, respectively.

Figure 2(B) shows water content and LOI profiles from cores 13B and 16B of clayey silts and silty clays on the lower slope. Water content decreases from 50–60% at the surface to about 40% at 20 cm depth, below which it becomes nearly constant. The LOI values are fairly uniform at about 7% for core 13B. The values for core 16B are a bit lower probably because of the sand content (5–10%) of this core. In general, water contents increase on the lower slope toward the South Okinawa Trough and away from land. LOI values show a similar trend.

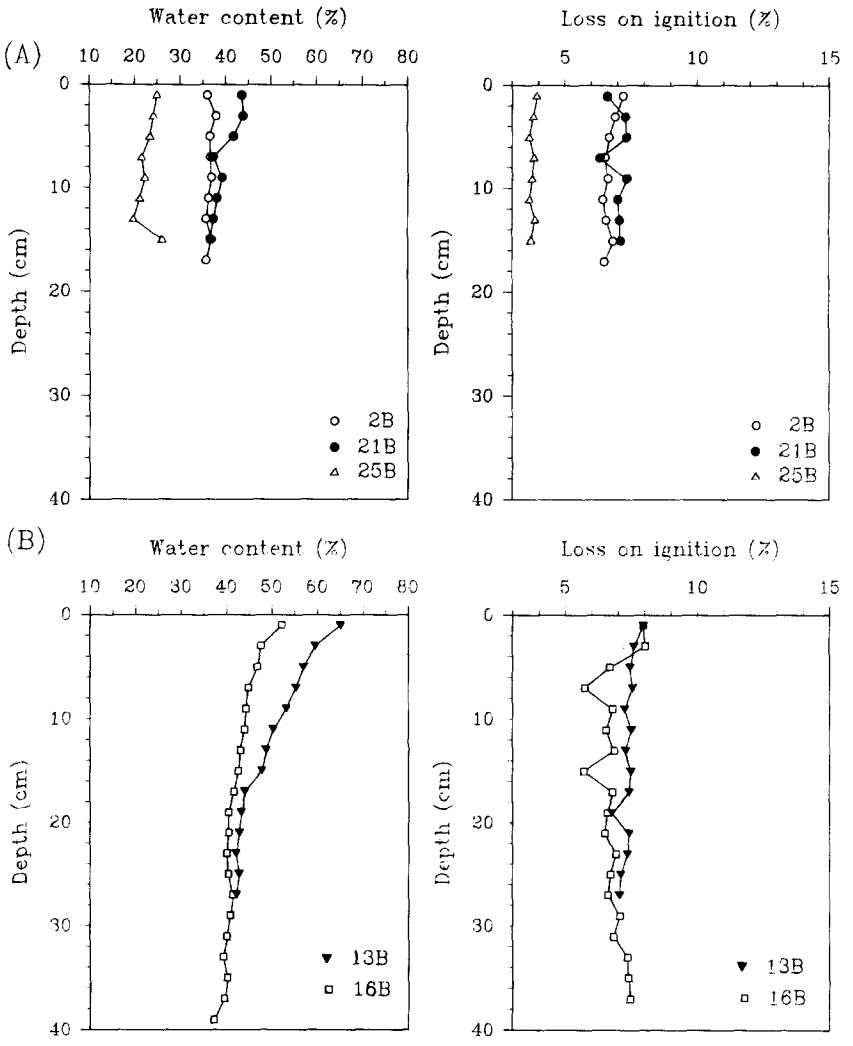

Fig. 2. Profiles of the water content and loss on ignition (LOI) from cores 2B, 21B and 25B (A), and from 13B and 16B (B).

Ra-226 *and* Pb-210 *activities: sedimentation rates*

The results of total Pb-210 and Ra-226 measurements together with the excess Pb-210 data are listed in Table 2. Ra-226 values are relatively unvarying downcore, typically between 0.5 and 2 dpm g^{-1}. In cores 2B and 21B, excess Pb-210 is present only in the top 2 cm. Ra-226 was not measured in core 25B, and the observed Pb-210 values are the lowest among all the cores studied. Excess and Ra-supported Pb-210 activities are highest in the fine-grained cores (silt and clay) from the lower slope.

Figures 3 and 4 show representative profiles of Pb-210 and Ra-226 activities used to calculate sedimentation rates. In some cores, a surface mixed layer of uniform Pb-210 activity is present. The downcore decay in excess Pb-210 activity yields sedimentation rates of 0.09–0.52 cm y^{-1}, or 0.08–0.42 g cm^{-2} y^{-1} (Table 3). The highest sedimentation rates

Table 2. Total Pb-210, Ra-226 *and excess* Pb-210 *data from the box cores studied. Values are decay-corrected, see footnotes*

Core depth (cm)	Total Pb-210† (dpm g^{-1})	Ra-226 (dpm g^{-1})	Excess Pb-210† (dpm g^{-1})
Core 2B			
0 ~ 2	1.48 ± 0.26	1.25 ± 0.03	0.23 ± 0.26
2 ~ 4	0.63 ± 0.23*	1.16 ± 0.04	—
4 ~ 6	1.13 ± 0.27*	1.06 ± 0.04	—
6 ~ 8	0.04 ± 0.27*	0.94 ± 0.04	—
8 ~ 10	0.80 ± 0.10*	0.81 ± 0.03	—
10 ~ 12	0.86 ± 0.07*	1.48 ± 0.05	—
12 ~ 14	0.97 ± 0.23*	2.15 ± 0.06	—
14 ~ 16	1.04 ± 0.10*	1.65 ± 0.05	—
16 ~ 18	1.04 ± 0.12*	1.15 ± 0.04	—
Core 5B			
0 ~ 2	56.20 ± 1.59	0.91 ± 0.03	55.29 ± 1.59
2 ~ 4	60.95 ± 1.67	1.30 ± 0.05	59.65 ± 1.67
4 ~ 6	91.33 ± 0.85	1.69 ± 0.07	89.64 ± 0.85
6 ~ 8	46.72 ± 1.08	1.74 ± 0.07	44.98 ± 1.08
8 ~ 10	52.43 ± 0.40	1.79 ± 0.07	50.64 ± 0.39
12 ~ 14	16.63 ± 0.59	0.42 ± 0.03	16.21 ± 0.59
16 ~ 18	7.19 ± 0.17	0.97 ± 0.05	6.22 ± 0.16
20 ~ 22	2.08 ± 0.66	1.52 ± 0.07	0.56 ± 0.66
26 ~ 28	1.28 ± 0.07*	1.50 ± 0.04	—
32 ~ 34	1.18 ± 0.17	1.14 ± 0.03	0.04 ± 0.17
38 ~ 40	0.65 ± 0.26*	0.78 ± 0.03	—
Core 6B			
0 ~ 2	60.71 ± 0.94	1.58 ± 0.06	59.13 ± 0.94
2 ~ 4	57.00 ± 0.72	1.34 ± 0.06	55.67 ± 0.72
4 ~ 6	58.94 ± 1.77	1.09 ± 0.06	57.85 ± 1.77
6 ~ 8	57.10 ± 1.43	1.21 ± 0.06	55.90 ± 1.43
8 ~ 10	37.41 ± 0.57	1.32 ± 0.06	36.09 ± 0.57
10 ~ 12	36.59 ± 0.23	1.19 ± 0.05	35.40 ± 0.22
12 ~ 14	30.40 ± 0.46	1.06 ± 0.04	29.34 ± 0.46
14 ~ 16	33.14 ± 0.31	0.99 ± 0.04	32.15 ± 0.31
16 ~ 18	22.96 ± 0.29	0.92 ± 0.05	22.04 ± 0.29
18 ~ 20	20.09 ± 0.43	1.06 ± 0.06	19.03 ± 0.43
22 ~ 24	17.00 ± 0.46	1.19 ± 0.07	15.81 ± 0.45
26 ~ 28	10.85 ± 0.48	1.04 ± 0.06	9.81 ± 0.48
32 ~ 34	4.94 ± 0.39	0.88 ± 0.04	4.06 ± 0.39
38 ~ 40	3.03 ± 0.26	1.16 ± 0.06	1.87 ± 0.25
Core 7B			
0 ~ 2	48.37 ± 0.24	1.08 ± 0.05	47.29 ± 0.23
2 ~ 4	47.86 ± 1.09	0.98 ± 0.05	46.88 ± 1.09
4 ~ 6	47.14 ± 0.32	0.88 ± 0.04	46.26 ± 0.32
6 ~ 8	35.70 ± 0.15	0.54 ± 0.03	35.16 ± 0.15
8 ~ 10	30.54 ± 1.21	0.20 ± 0.02	30.34 ± 1.21
10 ~ 12	30.02 ± 0.46	0.54 ± 0.03	29.48 ± 0.46
12 ~ 14	23.55 ± 0.52	0.88 ± 0.05	22.67 ± 0.52
14 ~ 16	24.31 ± 1.33	0.80 ± 0.05	23.51 ± 1.33
16 ~ 18	18.49 ± 0.78	0.72 ± 0.04	17.77 ± 0.78

continued

Table 2. Continued

Core depth (cm)	Total Pb-210† (dpm g^{-1})	Ra-226 (dpm g^{-1})	Excess Pb-210† (dpm g^{-1})
Core 7B			
18 ~ 20	12.28 ± 0.23	0.64 ± 0.04	11.64 ± 0.23
20 ~ 22	17.33 ± 0.58	0.56 ± 0.03	16.77 ± 0.58
22 ~ 24	16.78 ± 0.23	0.58 ± 0.04	16.20 ± 0.23
24 ~ 26	16.52 ± 0.69	0.60 ± 0.04	15.92 ± 0.69
26 ~ 28	11.29 ± 0.39	0.62 ± 0.04	10.67 ± 0.39
28 ~ 30	11.84 ± 0.27	0.64 ± 0.04	11.20 ± 0.27
30 ~ 32	8.10 ± 0.36	0.66 ± 0.04	7.44 ± 0.36
32 ~ 34	7.91 ± 0.08	0.68 ± 0.04	7.23 ± 0.07
34 ~ 36	8.35 ± 0.30	0.69 ± 0.04	7.66 ± 0.30
36 ~ 38	6.00 ± 0.71	0.71 ± 0.03	5.29 ± 0.71
Core 9B			
0 ~ 2	88.16 ± 0.68	1.25 ± 0.05	86.91 ± 0.68
2 ~ 4	75.74 ± 2.54	1.28 ± 0.05	74.46 ± 2.54
4 ~ 6	56.83 ± 0.88	1.31 ± 0.05	55.52 ± 0.88
6 ~ 8	43.23 ± 0.91	1.10 ± 0.04	42.13 ± 0.91
8 ~ 10	37.54 ± 1.33	0.89 ± 0.03	36.65 ± 1.33
12 ~ 14	24.06 ± 0.77	1.33 ± 0.04	22.73 ± 0.77
16 ~ 18	13.80 ± 0.69	0.82 ± 0.02	12.98 ± 0.69
20 ~ 22	5.18 ± 0.43	1.01 ± 0.03	4.17 ± 0.43
24 ~ 26	4.40 ± 0.21	0.96 ± 0.03	3.44 ± 0.21
28 ~ 30	5.31 ± 0.20	0.91 ± 0.04	4.40 ± 0.20
34 ~ 36	1.70 ± 0.18	1.53 ± 0.08	0.17 ± 0.16
Core 10B			
0 ~ 2	55.84 ± 1.64	1.22 ± 0.06	54.62 ± 1.64
2 ~ 4	66.39 ± 0.37	2.06 ± 0.06	64.34 ± 0.37
4 ~ 6	42.20 ± 0.88	2.89 ± 0.07	39.31 ± 0.88
6 ~ 8	35.10 ± 0.78	2.36 ± 0.07	32.75 ± 0.78
8 ~ 10	15.12 ± 0.69	1.82 ± 0.07	13.30 ± 0.69
12 ~ 14	13.32 ± 0.37	1.36 ± 0.04	11.96 ± 0.37
16 ~ 18	3.83 ± 0.12	0.97 ± 0.04	2.86 ± 0.11
20 ~ 22	1.97 ± 0.24	1.14 ± 0.06	0.83 ± 0.23
24 ~ 26	0.91 ± 0.07*	1.25 ± 0.05	—
28 ~ 30	0.80 ± 0.35*	1.35 ± 0.04	—
34 ~ 36	0.56 ± 0.39*	0.61 ± 0.03	—
Core 11B			
0 ~ 2	58.83 ± 0.46	2.05 ± 0.06	56.78 ± 0.46
2 ~ 4	87.94 ± 0.55	2.11 ± 0.07	85.83 ± 0.55
4 ~ 6	27.90 ± 0.72	2.16 ± 0.08	25.74 ± 0.72
6 ~ 8	13.22 ± 0.70	2.71 ± 0.08	10.51 ± 0.70
8 ~ 10	9.12 ± 0.14	3.25 ± 0.08	5.87 ± 0.12
12 ~ 14	3.15 ± 0.18	1.68 ± 0.06	1.47 ± 0.17
16 ~ 18	2.20 ± 0.15	1.75 ± 0.06	0.45 ± 0.14
20 ~ 22	2.04 ± 0.37	1.82 ± 0.06	0.22 ± 0.37
24 ~ 26	1.46 ± 0.13	1.45 ± 0.04	0.01 ± 0.12
30 ~ 32	1.71 ± 0.16*	1.72 ± 0.06	—
Core 13B			
0 ~ 2	73.42 ± 0.87	1.47 ± 0.08	71.95 ± 0.87
2 ~ 4	63.07 ± 1.14	1.44 ± 0.07	61.63 ± 1.14
4 ~ 6	33.14 ± 0.14	1.40 ± 0.07	31.74 ± 0.12

continued

Table 2. Continued

Core depth (cm)	Total Pb-210† (dpm g^{-1})	Ra-226 (dpm g^{-1})	Excess Pb-210† (dpm g^{-1})
Core 13B			
6 ~ 8	14.08 ± 0.85	1.44 ± 0.07	12.64 ± 0.85
8 ~ 10	10.27 ± 0.35	1.48 ± 0.07	8.79 ± 0.34
10 ~ 12	4.93 ± 0.67	1.35 ± 0.07	3.58 ± 0.67
12 ~ 14	2.19 ± 0.13	1.21 ± 0.07	0.98 ± 0.11
14 ~ 16	1.16 ± 0.19	1.15 ± 0.06	0.01 ± 0.18
18 ~ 20	0.96 ± 0.09*	1.09 ± 0.06	—
22 ~ 24	1.10 ± 0.21*	1.14 ± 0.05	—
26 ~ 28	0.58 ± 0.21*	1.19 ± 0.05	—
Core 16B			
0 ~ 2	50.77 ± 1.31	1.00 ± 0.04	49.77 ± 1.31
2 ~ 4	52.12 ± 1.45	0.88 ± 0.04	51.24 ± 1.45
4 ~ 6	41.80 ± 0.76	0.76 ± 0.03	41.04 ± 0.76
6 ~ 8	33.43 ± 0.36	0.84 ± 0.04	32.59 ± 0.36
8 ~ 10	28.95 ± 0.13	0.92 ± 0.06	28.03 ± 0.12
10 ~ 12	23.42 ± 0.58	0.74 ± 0.04	22.68 ± 0.58
12 ~ 14	20.26 ± 0.30	0.56 ± 0.03	19.70 ± 0.30
14 ~ 16	18.51 ± 0.78	0.67 ± 0.03	17.84 ± 0.78
16 ~ 18	13.33 ± 0.19	0.78 ± 0.04	12.55 ± 0.19
18 ~ 20	12.59 ± 0.40	0.76 ± 0.04	11.83 ± 0.40
20 ~ 22	13.92 ± 0.44	0.74 ± 0.04	13.18 ± 0.44
22 ~ 24	10.58 ± 0.80	0.72 ± 0.03	9.86 ± 0.80
24 ~ 26	8.51 ± 0.34	0.70 ± 0.03	7.81 ± 0.34
26 ~ 28	8.23 ± 0.44	0.68 ± 0.03	7.54 ± 0.44
28 ~ 30	5.63 ± 0.18	0.67 ± 0.03	4.96 ± 0.18
30 ~ 32	5.52 ± 0.40	0.65 ± 0.03	4.87 ± 0.40
32 ~ 34	5.99 ± 0.57	0.70 ± 0.02	5.29 ± 0.57
34 ~ 36	3.67 ± 0.34	0.75 ± 0.02	2.92 ± 0.34
36 ~ 38	2.98 ± 0.08	0.79 ± 0.02	2.18 ± 0.08
38 ~ 40	3.13 ± 0.48	0.84 ± 0.01	2.29 ± 0.48
Core 21B			
0 ~ 2	2.53 ± 0.52	0.97 ± 0.05	1.56 ± 0.52
2 ~ 4	1.02 ± 0.10*	1.16 ± 0.04	—
4 ~ 6	0.77 ± 0.12*	1.35 ± 0.04	—
6 ~ 8	0.70 ± 0.13*	1.37 ± 0.05	—
8 ~ 10	0.75 ± 0.03*	1.39 ± 0.06	—
10 ~ 12	0.60 ± 0.09*	1.41 ± 0.06	—
12 ~ 14	1.04 ± 0.17*	1.42 ± 0.06	—
14 ~ 16	0.37 ± 0.13*	1.44 ± 0.07	—
Core 25B			
0 ~ 2	0.71 ± 0.31*		
2 ~ 4	0.29 ± 0.24*		
4 ~ 6	0.21 ± 0.45*		
6 ~ 8	0.62 ± 0.33*		
8 ~ 10	0.63 ± 0.05*		
10 ~ 12	0.43 ± 0.40*		
12 ~ 14	0.56 ± 0.46*		
14 ~ 16	0.28 ± 0.31*		

*Observed value.
†Values corrected back to time of coring.

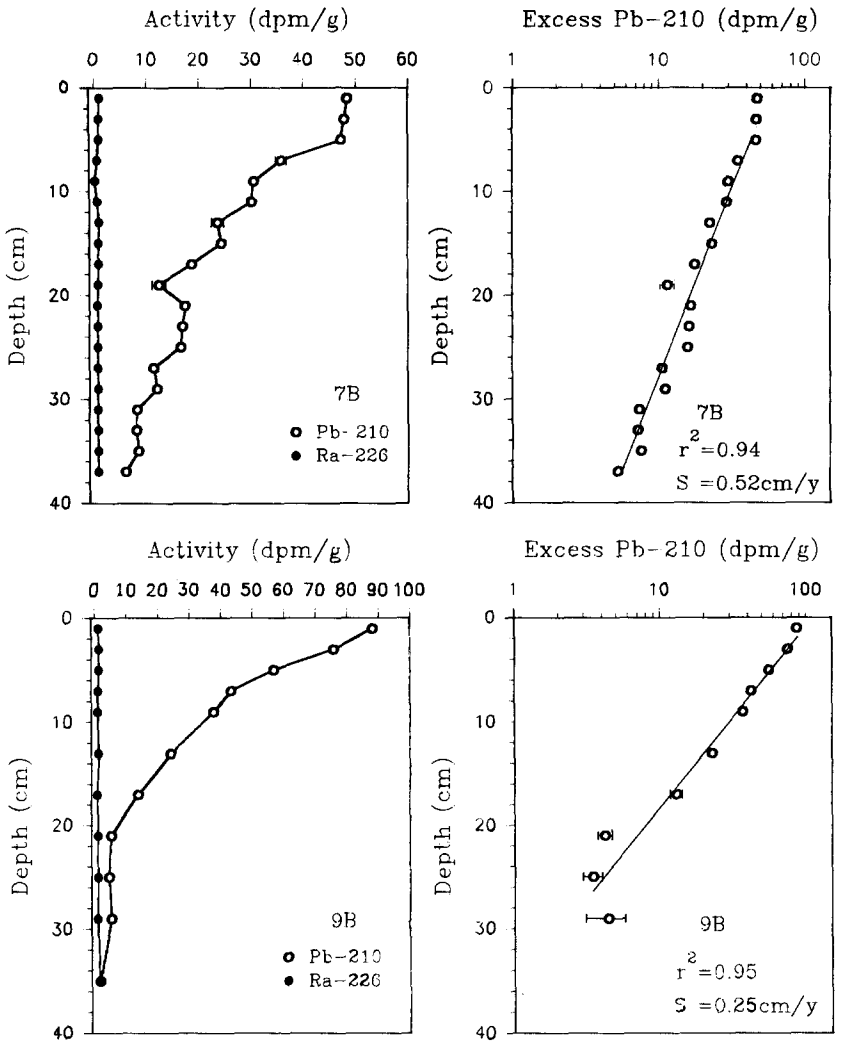

Fig. 3. Total Pb-210 and Ra-226 profiles from cores 7B and 9B. Excess Pb-210 data in log scale are fitted for sedimentation rate as indicated.

are located near Taiwan and decrease rapidly eastward (0.5 to 0.1 cm y^{-1} in 50 km) as the water depth increases toward the South Okinawa Trough (Fig. 5).

Excess Pb-210 *inventories and fluxes*

The excess Pb-210 inventories and fluxes for the cores studied are listed in Table 3 and shown in Fig. 6. Although the excess Pb-210 may extend beyond the core length in some cores (6B, 7B, 16B), the inventory or flux due to this contribution is estimated to be small (<5%) and so does not affect our interpretations.

Figure 6 shows two distinct groups of the excess Pb-210 inventories: one with values just over 300 dpm cm^{-2} on the east toward the trough (10B, 11B, 13B); the other with values

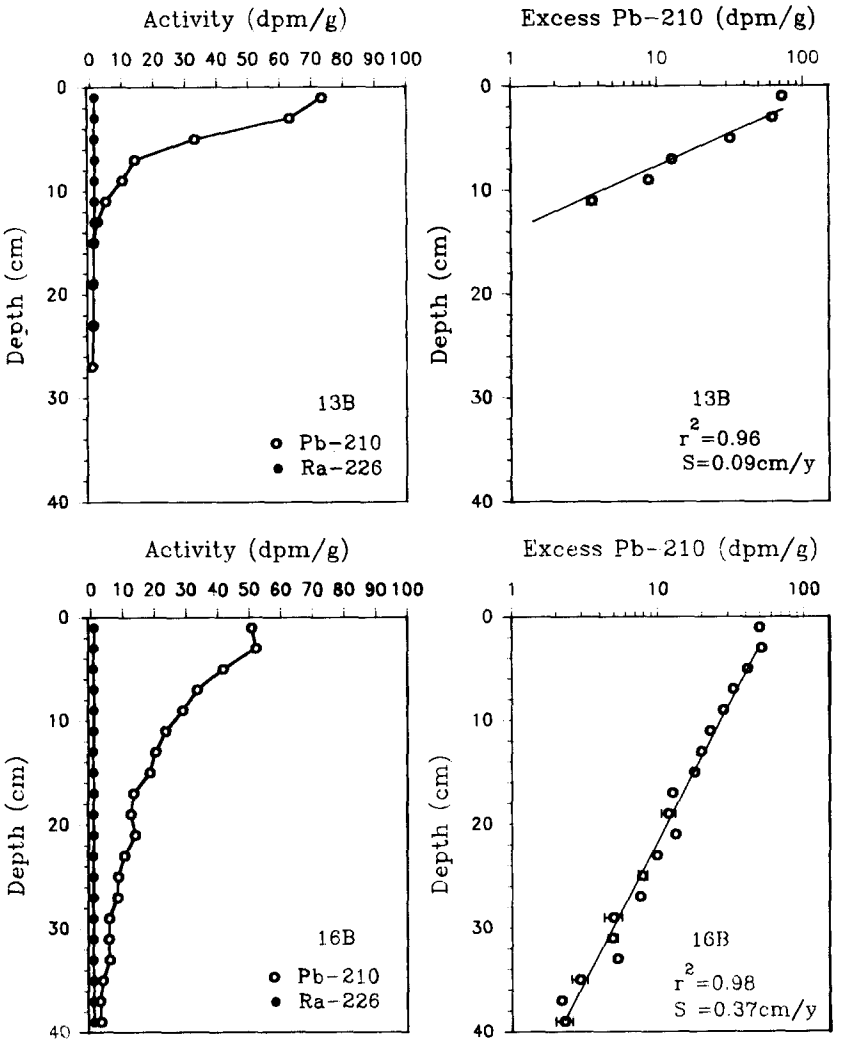

Fig. 4. Total Pb-210, Ra-226 profiles from cores 13B and 16B. Excess Pb-210 data in log scale are fitted for sedimentation rate as indicated.

over 600 dpm cm^{-2} on the west toward the Island, with a maximum over 800 dpm cm^{-2} (6B). The Pb-210 flux values, calculated from the inventory assuming a steady-state, also are divisible into two groups—one at about 10 dpm $cm^{-2}\,y^{-1}$ and the other at 20 dpm $cm^{-2}\,y^{-1}$.

DISCUSSION

Lithology in relation to water content and LOI

Water content and LOI provide a rough and rapid indication of the lithology. Coarse-grained sediments or sands usually have low water content and LOI; fine-grained

Table 3. Inventory and flux of excess Pb-210 *and sedimentation rate obtained from the box cores studied*

Core No.	Density (g cm^{-3})*	Sedimentation rate (cm y^{-1})	Sedimentation rate (g cm^{-2} y^{-1})	Excess Pb-210 inventory (dpm cm^{-2})	Excess Pb-210 flux (dpm cm^{-2} y^{-1})
2B	1.07	—	—	—	—
5B	0.86	0.10	0.086	636	19.8
6B	0.87	0.31	0.270	842	26.2
7B	0.81	0.52	0.421	662	20.6
9B	0.82	0.25	0.205	672	20.9
10B	0.77	0.10	0.077	374	11.6
11B	0.88	0.10	0.088	338	10.5
13B	0.84	0.09	0.076	322	10.0
16B	0.96	0.37	0.355	665	20.7
21B	1.05	—	—	—	—
25B	1.50	—	—	—	—

*Dry bulk density used for inventory calculation is defined as dry sediment wt./wet sediment volume. Values are from Lin (1992).

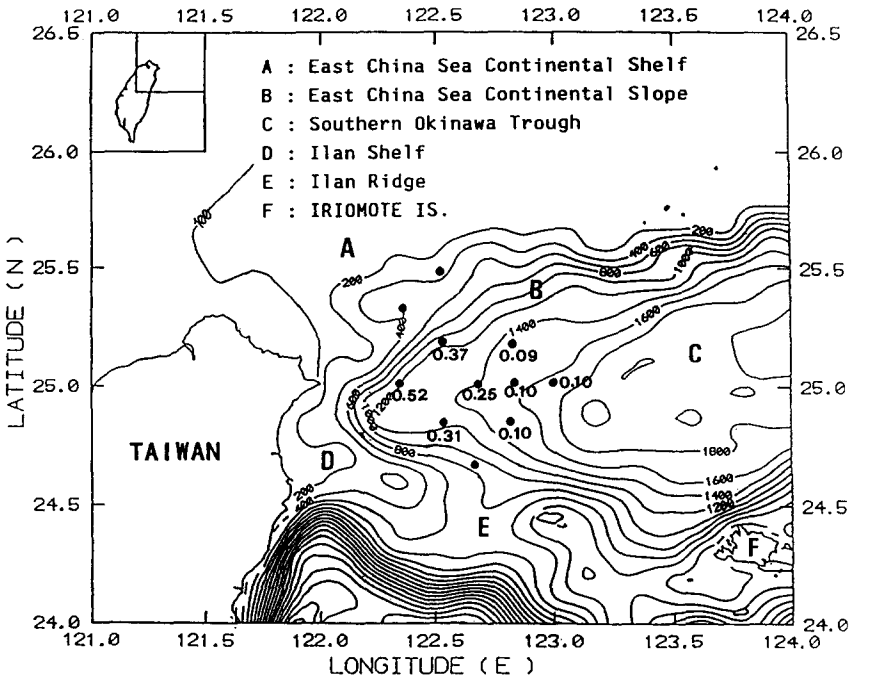

Fig. 5. Sedimentation rates (cm y^{-1}) calculated from excess Pb-210 profiles of the cores studied.

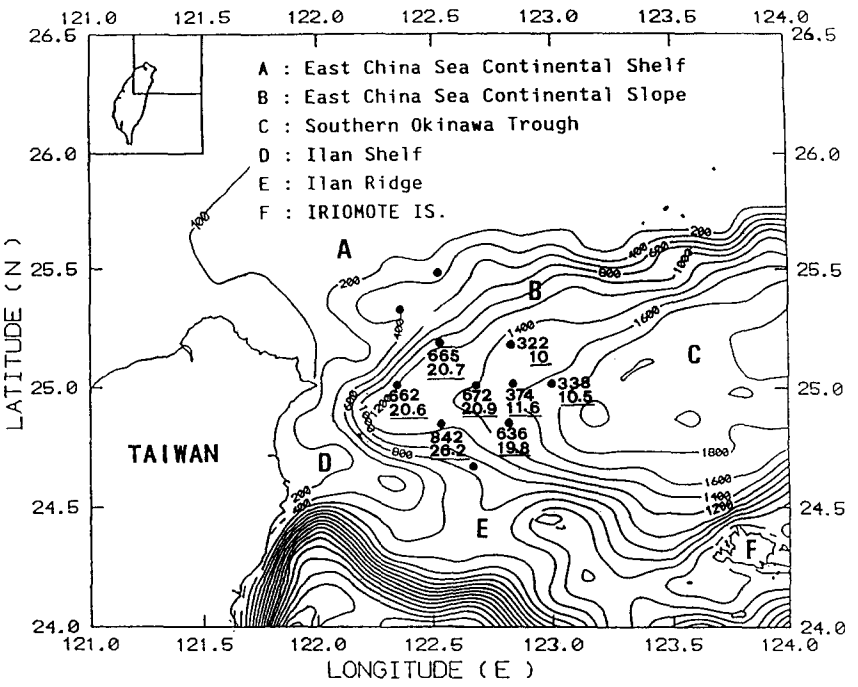

Fig. 6. Excess Pb-210 inventories (dpm cm^{-2}) and fluxes (dpm cm^{-2} y^{-1}) calculated from the excess Pb-210 profiles. The flux values are underlined.

sediments such as silts and clays have high water content and LOI. This rule applies well to the cores studied: the relict sediments of sand and pebble observed in core 25B on the upper slope have very low water content (<25%) and LOI (~4%); the fine-grained but poorly sorted silts and clays observed in 2B and 21B on the middle slope have intermediate water content (~40%) and high LOI (~7%); the fine-grained sediments in lower slope cores display the highest water content (~60% at surface and decreasing to ~40% below 20 cm) and high LOI (~7%). Within the lower slope of essentially fine-grained sediments, the increase in water content and LOI eastward with water depth toward the trough, probably results from the decrease in terrigenous sand.

Sources of Pb-210

In an area where horizontal transport is negligible, the Pb-210 flux to the sediments should be equal to the atmospheric Pb-210 flux plus the difference between Pb-210 production rate from Ra-226 decay and Pb-210 decay rate in the overlying water column under a steady-state condition. The atmospheric flux has been estimated at about 2 dpm cm^{-2} y^{-1} (NOZAKI and TSUNOGAI, 1973; TUREKIAN *et al.*, 1977). TSUNOGAI *et al.* (1985) measured a flux of about 1.6 dpm cm^{-2} y^{-1} in Okinawa. It is not clear whether this difference is a latitudinal effect. The production rate from Ra-226 decay in the western South Okinawa Trough is estimated to be about 0.6 dpm cm^{-2} y^{-1} for a water column of 1500 m based on some Ra-226 profiles measured in the same region (CHUNG and YIN, in preparation). The Pb-210 decay rate for the same water column is about 0.2 dpm cm^{-2} y^{-1}

(excluding atmospheric input) based on a Pb-210 profile measured in the area (YANG and LIN, 1992). Thus, the expected Pb-210 flux onto the sediments in the area should be about 2–3 dpm cm^{-2} y^{-1}. Actual fluxes calculated from the inventory range (Fig. 6) are about 5–13 times the expected vertical flux. The source or sources of such a large excess must be sought. Two alternative explanations are considered: (1) boundary scavenging of Pb-210 at the sediment–water interface similar to that proposed by BACON *et al.* (1976) coupled with Kuroshio advection; or (2) lateral or downslope transport of high Pb-210 activity fine-grained sediments.

Boundary scavenging. The boundary scavenging process proposed by BACON *et al.* (1976) requires a combination of variable horizontal diffusion and first-order (concentration dependent) *in situ* scavenging by particles. Since most cores in the present study are located on the lower slope close to the trough (Fig. 1), potential Pb-210 source area is confined to the trough and cannot account for the observed Pb-210 flux. As the area is within the Kuroshio path, north- or northeastward advection probably dominates over horizontal diffusion. Thus boundary scavenging of Pb-210 may be enhanced by advection of Kuroshio water from the south.

To evaluate the above interpretation, it is necessary to estimate the source and scavenging efficiency of Pb-210 advected into this slope area. To the south of the study area, the Ilan ridge has a sill depth of about 800 m. The water column above this depth has a mean Pb-210 concentration of about 12 dpm 100 kg^{-1} or 120 dpm m^{-3} (LIN and CHUNG, 1991). This value is almost identical to the mean Ra-226 concentration for the same water column (126 dpm m^{-3}) (LIN and CHUNG, 1991). However, Pb-210 is in excess over Ra-226 supported levels in the upper 250 m–450 m due to the atmospheric flux, but it decreases to less than Ra-226 below this depth due to particulate scavenging (LIN and CHUNG, 1991).

If the slope area is about 1×10^4 km^2 with an average water depth of 1500 m, then the total water volume is about 1.5×10^{13} m^3. Although the velocity and transport of the Kuroshio east of Taiwan are quite variable (CHU, 1970, 1974), maximum velocities range between 30 and 120 cm s^{-1}. Using an average northward advection of 50 cm s^{-1} for the layer in question, the fluid transport through the area is about 4×10^7 m^3 s^{-1} (or 40 Sv). Because velocity profiles of the Kuroshio in the area are lacking, this transport value is subject to a large uncertainty, but is in agreement with that obtained previously by CHERN (1983) and LIU (1983) in the same area, based on hydrography and some current measurements. This yields a mean residence time of 4.3 days for the Kuroshio water advected through the area. The Pb-210 available for removal by particulate and boundary scavenging is about 1514 dpm cm^{-2} y^{-1}. To account for the Pb-210 flux of 10 to 26 dpm cm^{-2} y^{-1} (Fig. 6), a scavenging efficiency of 0.7–1.7% is necessary. As the particulate scavenging of Pb-210 in open ocean is at least 10% (e.g. THOMSON and TUREKIAN, 1976), such a small efficiency of boundary scavenging is quite feasible.

Downslope transport of fine-grained sediments. The other possibility for causing the excessive Pb-210 flux on the lower slope is lateral or downslope transport of high Pb-210 activity sediments from the continental shelf and upper slope by bottom and tidal currents. WU (1992) found a strong bottom tidal current trending NW–SE in the Mien Hua Submarine Canyon (25°25'N, 122°7'E) near core 21B. Northeast of the canyon, a counter-current flows southwestward along the 300 m contour line (CHUANG and WU, 1991) west of the northeastward flowing Kuroshio. Therefore fine-grained sediments originating from

the East China Sea as well as those from the Taiwan shelf might be transported down the upper and middle slope via valleys and channels by tidal currents and then to the lower slope and the South Okinawa Trough by the southward counter current.

Sediments from the upper slope (core 25B) are coarse sands and gravels with negligible Pb-210 activity. Although sediments are fine-grained on the middle slope, they show little or no Pb-210 excess (cores 2B and 21B). As Pb-210 is primarily scavenged and transported by fine-grained particles and aggregates, the lack of excess Pb-210 suggests that these fine-grained sediments are old (>100 years), being exposed by recent erosion or simply no accumulation of fine-grained sediments in the past 100 years. This supports that the high Pb-210 particles just bypass the middle slope to the lower slope.

In the East China Sea shelf water, *in situ* Pb-210 production by Ra-226 decay in a 200 m water column is small (at most 0.06 dpm cm^{-2} y^{-1} with an average Ra-226 concentration of 10 dpm 100 kg^{-1}; CHUNG and YIN, in preparation) compared to the atmospheric flux of 1.6 dpm cm^{-2} y^{-1} (TSUNOGAI *et al.*, 1985). Additional input is supplied by river discharge of particulates into the East China Sea. Although the combined sources of Pb-210 from the East China Sea are probably less than 4 dpm cm^{-2} y^{-1}, our core data indicate that Pb-210 bypasses the shelf and upper–middle slope and is focused on the lower slope. A 10^4 km^2 area of the lower slope is the depositional site for a shelf area seven times as large (7×10^4 km^2)—about 10% of the East China Sea shelf. Thus Pb-210 inventories on the lower slope, and to some extent the South Okinawa Trough, may be provided by the atmospheric and riverine input from the East China Sea Shelf.

CONCLUSIONS

Excess Pb-210 inventory and flux may be used as a tracer of particle dynamics on the lower continental margin, in addition to a determination of 100 years sedimentation rates. Cores taken from the continental slope between northern Taiwan and the South Okinawa Trough indicate that: (1) Pb-210 flux into the lower slope between 900 m and 1600 m depth is extremely high, ranging from 10 to 26 dpm cm^{-2} y^{-1}, about 4–10 times that observed by NARITA *et al.* (1990) in the South Okinawa Trough (>2000 m); (2) little or no Pb-210 is observed on the upper and middle slope due to the absence of fine-grained sediment accumulation; (3) sedimentation rates on the lower slope as determined from excess Pb-210 profiles range between 0.09 and 0.52 cm y^{-1} (0.08–0.42 g cm^{-2} y^{-1}). These rates are about two to three orders of magnitude higher than those commonly observed in the abyssal plain (e.g. GOLDBERG and KOIDE, 1962; CHEN and CHUNG, 1990).

The excessive flux of Pb-210 on the lower slope may be interpreted in two ways; as boundary scavenging associated with Kuroshio flow, or lateral (downslope) transport of fine-grained sediments. The first interpretation requires only about 0.7–1.7 % of the Pb-210 in the Kuroshio water above 800 m depth to be scavenged from the water column, and so is easily feasible. The second interpretation requires lateral transport of fine-grained sediments from the shelf and upper–middle slope to the lower slope. This mechanism is supported by presence of relict sediments in the shelf and lack of Pb-210 on the upper–middle slope. The sedimentation rates decrease toward the east on the lower slope. Transport may occur by tidal and/or bottom currents in channels and valleys incising the slope. Pb-210 inventories on the lower slope would require supply from about 10% of the East China Sea shelf. Currents patterns on the upper slope and counter currents west of the Kuroshio are consistent with this interpretation.

Acknowledgements—We wish to thank professor M.P. Chen and technicians on board the R.V. *Ocean Researcher I*, who ably collected all the box cores used for this study. We also appreciate the help of the crew and assistants during the sampling cruise. Miss L. C. Hung of our laboratory has provided a great assistance in typing and word-processing the manuscript.

Two anonymous reviewers' critical comments are most helpful in revising and improving the manuscript.

Financial support has been provided by the National Science Council for our participation in the KEEP (Kuroshio Edge Exchange Processes) programs in the last several years (NSC 79-0209-M-110-02; NSC 80-0209-M-110-06; NSC 81-0209-M-110-04; NSC 82-0209-M-110-043-K).

REFERENCES

Applequist, M. D. (1975) Lead-210 in the deep sea: Pacific Ocean investigations. M. S. Thesis, University of California, San Diego, California, 127 pp.

Bacon, M. P., D. W. Spencer and P. G. Brewer (1976) Pb-210/Ra-226 and Po-210/Pb-210 disequilibria in seawater and suspended particulate matter. *Earth and Planetary Science Letters*, **32**, 277–296.

Boggs S. Jr, W. C. Wang, F. S. Lewis and J. C. Chen (1979) Sediment properties and water characteristics of the Taiwan shelf and slope. *Acta Oceano Taiwanica*, **10**, 10–49.

Broecker, W. S., J. Goddard and J. Sarmiento (1976) The distribution of Ra-226 in the Altantic Ocean. *Earth and Planetary Science Letters*, **32**, 220–235.

Chen M. P. (1983) Physical properties and depositional environments of continental slope sediments, southern Taiwan strait. *Acta Oceanographica Taiwanica*, **14**, 42–63.

Chen M. P. and M Covey (1983) Radiocarbon dating of piston cored sediments from the Taiwan strait: preliminary results. *Acta Oceanographica Taiwanica*, **14**, 9–15.

Chen M. P., S. C. Lo and K. L. Lin (1992) Composition and texture of surface sediment indicating the depositional environments off Northeast Taiwan. *Terrestrial, Atmospheric and Oceanic Sciences*, **3**, 395–416.

Chen R. S. and Y. Chung (1990) Sedimentation rates in the western Philippine Sea. *Terrestrial, Atmospheric and Oceanic Sciences*, **1**, 111–125.

Chern C. S. (1983) On the characteristics of current at the offshore region of Suao. *Acta Oceanographica Taiwanica*, **14**, 75–87.

Chu T. Y. (1970) *Report on the variation of velocity and volume transport of the Kuroshio*. First Symposium of CSK, Honolulu, pp. 163–174.

Chu T. Y. (1974) The fluctuations of the Kuroshio current in the eastern sea area of Taiwan. *Acta Oceano Taiwanica*, **4**, 1–10.

Chuang W. S. and C. K. Wu (1991) Slope current fluctuations northeast of Taiwan, Winter 1990. *Journal of the Oceanography Society of Japan*, **47**, 185–193.

Chung Y. (1971) Pacific deep and bottom water studies based on temperature, radium and excess-radon measurements, Ph. D. Thesis, University of California, San Diego, 239 pp.

Chung Y. and H. Craig (1980) Radium-226 in the Pacific Ocean, *Earth and Planetary Science Letters*, **49**, 267–293.

Chung Y. and H. C. Yin (in preparation) Radium-226 in the Kuroshio near Taiwan: some preliminary results from the KEEP and KEEP-MASS programs.

Goldberg E. D. and M. Koide (1962) Geochronological studies of deep sea sediments by the ionium/thorium method. *Geochimica et Cosmochimica Acta*, **26**, 417–450.

Ho C. S. (1986) A synthesis of the geologic evolution of Taiwan. *Memo. Geol. Soc. China*, **7**, 15–29.

Ku T. L., C. A. Huh and P. S. Chen (1980) Meridional distribution of Ra-226 in the eastern Pacific along GEOSECS cruise tracks. *Earth and Planetary Science Letters*, **49**, 293–308.

Li Y. H. (1976) Denudation of Taiwan Island since the Pliocene Epoch. *Geology*, **4**, 105–107.

Lin K. L. (1992) Sedimentary structure, texture and clay minerals of surficial sediments off northeastern Taiwan. M. S. Thesis, National Taiwan Univ., 93 pp.

Lin F. J. and J. C. Chen (1983) Textural and mineralogical studies of sediments from the southern Okinawa trough, *Acta Oceanologica Taiwanica*, **14**, 26–41.

Lin Y. N. and Y. Chung (1992) Pb-210 and Po-210 distributions and their radioactive disequilibria in the Kuroshio waters off eastern and northeastern Taiwan. *Terrestrial, Atmospheric and Oceanic Sciences*, **2**, 243–265.

LIN S., K. K. LIU, M. P. CHEN, P. CHEN and F. Y. CHANG (1992) Distribution of organic carbon in the KEEP area continental margin sediments. *Terrestrial, Atmospheric and Oceanic Sciences*, **3**, 365–376.

LIU C. T. (1983) As the Kuroshio turns: (I) Characteristics of the current. *Acta Oceanographica Taiwanica*, **14**, 88–95.

LIU K. K., G. C. GONG, S. LIN, C. Y. YANG, C. L. WEI, S. C. PAI and C. K. WU (1992) The year-round upwelling at the shelf break near the northern tip of Taiwan as evidenced by chemical hydrography. *Terrestrial Atmospheric and Oceanic Sciences*, **3**, 243–276.

NARITA H., K. HARADA and S. TSUNOGAI (1990) Lateral transport of sediment particles in the Okinawa Trough determined by natural radionuclides. *Geochemical Journal*, **24**, 207–216.

NOZAKI Y. and S. TSUNOGAI (1973) Lead-210 in the north Pacific and the transport of terrestrial material through the atmosphere. *Earth and Planetary Science Letters*, **20**, 88–92.

THOMSON J. and K. K. TUREKIAN (1976) ^{210}Po and ^{210}Pb distributions in oceanwater profiles from the eastern South Pacific. *Earth and Planetary Science Letters*, **32**, 297–303.

TSAI S. W. and Y. CHUNG (1989) Pb-210 in the sediments of Taiwan Strait. *Acta Oceanographica Taiwanica*, **22**, 1–13.

TSUNOGAI S., T. SHINAGAWA and T. KURATA (1985) Deposition of anthropogenic sulfate and Pb-210 on the western North Pacific area. *Geochemical Journal*, **19**, 77–90.

TUREKIAN K. K., Y. NOZAKI and L. K. BENNINGER (1977) Geo-chemistry of atmospheric radon and radon products. *Annual Review of Earth and Planetary Sciences*, **5**, 227–255.

WU C. K. (1992) On the characteristics of bottom tidal currents in northeast Taiwan. *Terrestrial, Atmospheric and Oceanic Sciences*, **3**, 293–304.

YANG C. Y. and H. C. LIN (1992) Lead-210 and polonium-210 across the frontal region between the Kuroshio and the Each China Sea, northeast of Taiwan. *Terrestrial, Atmospheric and Oceanic Sciences*, **3**, 379–393.

YU H. S. and E. HONG (1992) Physiographic characteristics of the continental margin, northeast Taiwan. *Terrestrial, Atmospheric and Oceanic Sciences*, **3**, 419–433.